DOI: 10.1002/ejoc.200701123

A Neutral DNA Sequence-Selective Vector for Interaction Studies: Fluorescence Binding Experiments Directed Towards a Carbohydrate-DNA Carrier

Pablo Peñalver,[a] Samadi Abdelouahid,[a] Paula Bosch,[b] Christopher A. Hunter,[c] and Cristina Vicent*[a]

Keywords: Carbohydrates / DNA recognition / Fluorescence spectroscopy / Vectors

The distamycin-type γ-linked covalent dimer -Py-γ-Py-Ind has been shown to be a neutral selective vector capable of transporting recognition elements to the minor groove of DNA for further structural studies. Comparison of fluorescence binding constants of the complexes formed by the vectors (R-Py-γ-Py-Ind **1** and **3**) with *ct*-DNA and *poly*(dA-dT) showed that -Py-γ-Py-Ind is a neutral (–ATAT–)-selective vector. We also provide experimental data that show that the vector can be used as a sugar-carrier to the DNA. Thus, modifying the vector at the C terminus with sugars of different configurations (**4**–**7** D vs. **8** L), and with both α- and β-linkages (**5** and **4**, respectively) to the oligoamide fragment provides efficient DNA binders ($K_a = 1.1 \times 10^4$ to 3.2×10^5 M^{-1}). Moreover, the sugar residue is able to modulate the binding to the different DNA polymers studied and, even more relevantly, the sugar contributes to the selectivity of binding: β-D-Gal-Py-γ-Py-Ind (**6**) is the most selective –ATAT–sugar–oligoamide ligand {$\Delta\Delta G°$ **6** [*poly*(dA-dT) – *ct*-DNA] = –4.0 kcal mol^{-1}}. We have used fluorescence quantum yield values to ensure the presence of similar free state conformation for ligands **1**–**8** and we can thus correlate the differences in the measured binding energies with the changes in the shape of the structural elements. Finally, we have demonstrated that the sequence-selective sugar carrier makes a 1:1 complex with the Drew–Dickerson oligonucleotide dodecamer, thus opening the road to more detailed structural and thermodynamic studies of sugar-oligoamide DNA short oligonucleotide complexes in solution.

Introduction

Over the past decades, the grooves of B-DNA have been used as relevant targets to interfere in DNA transcription.[1–6] There has been extensive progress on the design of small molecules capable of recognizing the minor groove of B-DNA,[5,6,7–12] while a more relevant goal, of course, was the design of compounds that could bind preferentially to a specific DNA sequence.[11,13–27]

In general, establishing the molecular basis of selective binding to the grooves of DNA presents difficulties. The general rule is to design molecules that might be able to make specific contacts through hydrogen bonds with the different H-bonding centres provided by the different nucleotide sequences in the grooves, helped by charge–charge interactions with the phosphate backbone and stabilized by hydrophobic contacts. Additionally, the conformation of the ligand should allow the molecule to surround the groove of DNA.[7,28–30]

Furthermore, DNA differs from other biological targets, such as proteins or RNA, in the lack of a "structurally well defined binding site". Sometimes, this fact makes the characterization of a single complex of a new DNA binder in solution difficult or impossible (multiple binding is difficult to avoid). It is therefore even more difficult to carry out structural studies that might provide information on the requirements of sequence-selective binding for use in de novo ligand design in the case of DNA than it is in cases of other biomolecules.

Carbohydrate components are present in many antibiotics and anticancer drugs that target DNA. Most of them are groove binders,[7,31–34] and in some cases the carbohydrate residue is responsible for sequence-selective binding of the drug. This is the case with the calicheamicin oligosaccharide, which selectively binds into the minor groove of DNA. The calicheamicin oligosaccharide has been extensively chemically modified because of its therapeutic relevance.[35] Thermodynamic and structural information relating to the complexes have provided information on the effects of its particular sugar modifications on binding.[36,37]

[a] Departamento de Química Orgánica Biológica, Instituto de Química Orgánica general, CSIC,
c/ Juan de la Cierva 3, 28006 Madrid, Spain
Fax: +34-91-564-48-53
E-mail: iqocv18@iqog.csic.es
[b] Dept. Polymer Photochemistry, Instituto de Ciencia y Tecnología de Polímeros, CSIC,
c/ Juan de la Cierva 3, 28006 Madrid, Spain
[c] Department of Chemistry, Krebs Institute for Biomolecular Science, University of Sheffield,
Sheffield S3 7HF, UK
Supporting information for this article is available on the WWW under http://www.eurjoc.org or from the author.

However, this approach presents limitations stemming from the necessity of maintaining the general structure of the sugar residue of the ligand and the difficulties inherent in the particularly complicated calicheamicin oligosaccharide synthesis.[38] Therefore, it does not allow drastic changes in the structure of the carbohydrate in order to explore new binding motifs without completely losing the interaction.

Additionally, the relevance of carbohydrate–DNA interaction is currently growing with recent advances in glycosciences. The characterization of nuclear *glycoproteins that act as transcription factors*[39–41] in which carbohydrate residues act as switches of the glycoprotein function is suggesting the importance of developing chemical tools to shed light on glyco-effects on glycoprotein–DNA interaction.

We are interested in developing a general strategy that would allow us to determine the molecular basis of carbohydrate–DNA binding. Initially we explored the use of carbohydrate hydrogen bonding cooperativity[42–45] to favour DNA binding and we characterised sugar H-bonding patterns that efficiently bind CG[46] and phosphate[47,48] in apolar solvents. In order to establish the efficiency of these binding elements to the biological target and under physiological conditions we first need to design a *vector molecule*: a compound that will bring our new designed binding motives to the minor groove of DNA without complete loss of interaction and binding sequence selectivity, hopefully to fix the carbohydrate to a unique binding site of a designed oligonucleotide. A well defined 1:1 complex would thus then be susceptible to structural and thermodynamic study in order to shed light on the basis of the interaction.

More recently, we described[49] the first results of this new strategy. The design of the sugar-oligoamide derivative involved taking into account that the *bound conformation* of distamycin-type γ-linked covalent dimers, as described by Wemmer et al.,[50] is a *hairpin conformation*. As a carrier selective towards a neutral carbohydrate DNA minor groove sequence we selected the side-by-side pairing of *N*-methyl-pyrrolecarboxamide (Py) units covalently joined head-to-tail through a flexible linker (γ-aminobutyric acid) as the minimum oligoamide fragment that would retain not only the binding ability but also, we hoped, the sequence specificity for the AT/TA sequence.[19,51,52] The sugar and an indole residue were then attached to the C terminus and the N terminus, respectively, of a -Py-γ-Py- chain to afford the sugar-oligoamides of the general structure (sugar-Py-γ-Py-Ind) (Scheme 1). The presence of the hairpin bound state conformation[53] in the free state should increase the binding, and the γ linker should help a 1:1 binding mode to the minor groove[54–56] and a preferred oligoamide orientation ($N_{terminus}$–$C_{terminus}$ orientates preferentially along the 5′–3′ direction of the DNA helix).[57,58]

The sugar-oligoamides **4**, **6** and **7** were therefore synthesized.[49] An nOe study suggested that the sugar-oligoamides each present a noticeable percentage of hairpin conformation in the free state, while TR-NOESY data also suggested hairpin structures in the bound state. Additionally, a qualitative study of the binding with *ct*-DNA by NMR showed specific interaction, while a competition experiment

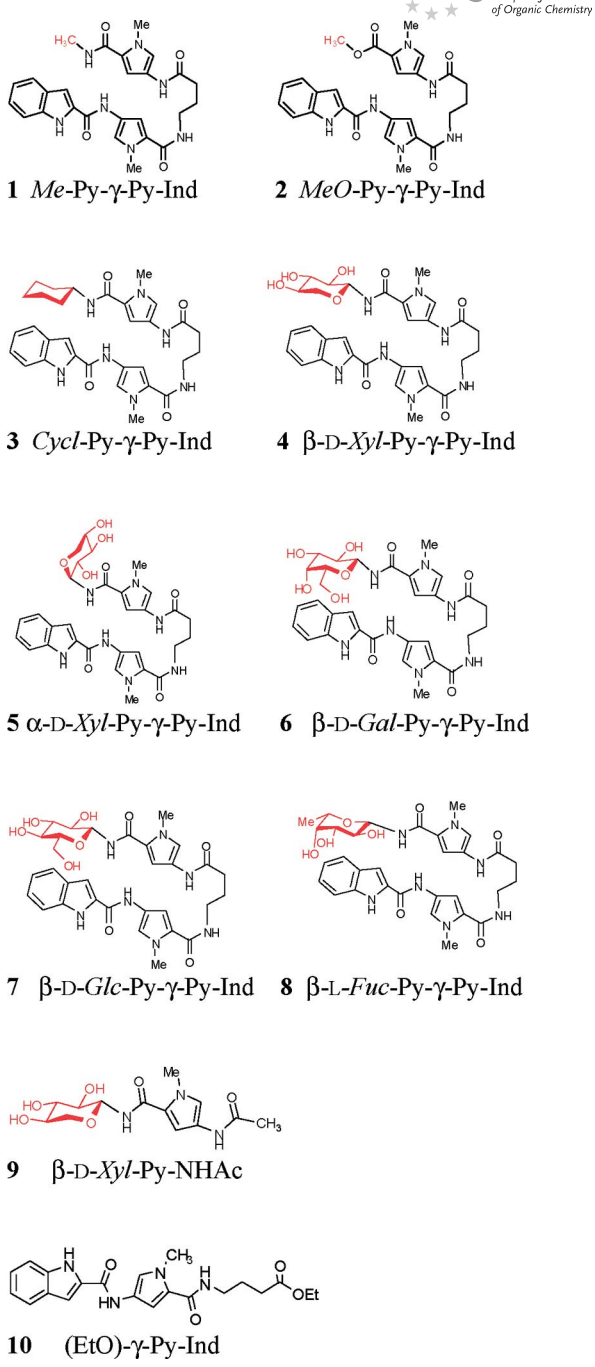

Scheme 1. Structure of vectors **1**–**3**, sugar-oligoamides **4**–**8** and models **9**–**10**.

with netropsin suggested that the designed ligands are minor groove binders.

We now have synthesized vector-oligoamides **1**–**3** and quantified their binding to *ct*-DNA, *ml*-DNA and *poly*(dA-dT) by fluorescence spectroscopy,[14,21,59,60] with the aim of confirming that the neutral oligoamide -Py-γ-Py-Ind residue (see Scheme 1) can be used as a selective sequence carrier for the DNA minor groove: **1** and **2** are non-carbohydrate oligoamides with their C termini represented by a methyl amide **1** and an ester linkage in methyl ester **2**, which are used to determine the minimal structure of the oligo-

amide vector with efficient binding. Additionally, the cyclohexyl derivative **3** is also a non-carbohydrate hydrophobic model with a steric volume similar to that of the sugar pyranose ring.

Also here for the first time, we have quantified and compared the binding to *ct*-DNA, *poly*(dA-dT), *ml*-DNA and *poly*(dC-dG) of sugar-oligoamide ligands with different configurations (**4**–**7** D vs. **8** L), and also with both α- and β-linkages (**4** and **5**, respectively) to the oligoamide fragment compounds.[61]

Results and Discussion

Fluorescence Characterization of the Ligands 1–10 in the Free State

As a first step, a study of the absorption and emission properties of the free ligands (assignment of the chromophores responsible for the fluorescence of the vector and sugar-oligoamides) was carried out (see Supporting Information, Figures S1 and S2).

The absorption and fluorescence properties of vectors **1**–**3**, sugar-oligoamides **4**–**8** and models **9**–**10**, as well as their molar extinction coefficients both in phosphate buffer solution and in phosphate buffer/DMSO mixtures, are summarized in Table S1 in the Supporting Information.

The study shows that the oligoamides **1**–**8** and (EtO)-γ-Py-Ind (**10**) all showed identical emission and excitation spectra. The bands at 280 nm and 295 nm were attributed to the fluorescence emission of the pyrrole and indole groups, respectively, once the model **9** had been fully characterised and the pyrrole fluorophore correctly assigned.

As expected, the fluorescence emission of the indole fluorophore is much more intense than that of the pyrrole one. We therefore selected the indole fluorophore maximum emission wavelength (λ = 410 nm) in order to follow the changes in the fluorescence emission intensity in the quantum yield measurements and DNA titration studies.[62]

In an earlier work from our group,[49] the hairpin conformations of sugar-oligoamides **4**, **6** and **7** in aqueous solution were characterized by NMR spectroscopy.[63]

Here, we have used fluorescence quantum yield values to ensure the presence of similar free state conformations for ligands **1**–**8** and thus to correlate the differences in the measured binding energies with the changes in the shape of the structural elements (Scheme 2).

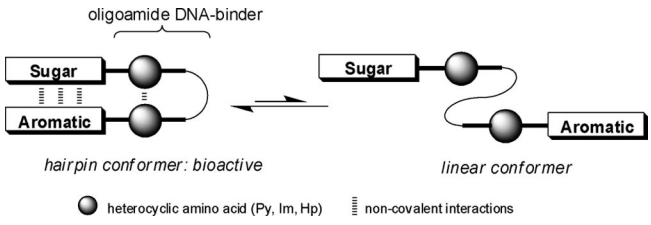

Scheme 2. Hairpin/linear conformers in equilibrium.

The fluorescence quantum yield (Φ_f) values of the indole fluorophore[60,64] for **4**–**8** and that of the structurally related indole-strand model **10**, the structure of which does not allow a hairpin conformation, are summarized in Table 1.

Table 1. Fluorescence quantum yield for ligands **4**–**8** and models **9**–**10** measured in buffer solution.

Ligands		$\Phi_f \times 10^{-3}$
β-D-Xyl-Py-γ-Py-Ind	**4**	3.44
α-D-Xyl-Py-γ-Py-Ind	**5**	5.49
β-D-Gal-Py-γ-Py-Ind	**6**	3.83
β-D-Glc-Py-γ-Py-Ind	**7**	3.71
β-L-Fuc-Py-γ-Py-Ind	**8**	3.49
β-D-Xyl-Py-NHAc	**9**	1.34 [a]
(EtO)-γ-Py-Ind	**10**	47.04
(EtO)-γ-Py-Ind + β-D-Xyl-Py-NHAc	**1**:**4**	17.78

[a] Not indole but pyrrole fluorophore.

(EtO)-γ-Py-Ind (**10**) has a fluorescence quantum yield value approx. 15 times higher than those of all the β-sugar-oligoamides **4**, **6**–**8**. This result is completely in agreement with the presence in solution of a hairpin conformation, which would allow intramolecular proximity between the sugar and the oligoamide and quench the fluorescence emission of the indole fluorophore.

Additionally, the fluorescence quantum yield of a 1:4 mixture of (EtO)-γ-Py-Ind (**10**) and β-D-Xyl-Py-NHAc (**9**) was measured. Interestingly, the quantum yield of the mixture was also decreased by more than 50% relative to that of (EtO)-γ-Py-Ind (**10**) alone. The effect can in this case be explained in terms of intermolecular interaction between both sugar- and indole-strand models favoured by the excess of sugar-strand **9**.

Even more relevantly to our studies, the quantum yield values for the sugar-oligoamides **4** and **6**–**8** containing sugar β-linkages to their oligoamide fragments are very similar in value, so we can assume that the proportions of hairpin conformation in solution are similar for all compounds and independent of the stereochemistry of the sugar. These fluorescence results are in agreement with NMR conformational evidence previously reported for **4**, **6** and **7**.[49] This should allow us to attribute the differences in the binding properties of the different sugar-oligoamides to the stereochemistry of the sugar present in the ligand and not to significant differences in free state conformations.

In an effort to obtain additional experimental evidence relating to the conformational differences of the general hairpin structures depending on the anomeric configurations in the sugar-oligoamides,[49] we also investigated the fluorescence properties of α-D-Xyl-Py-γ-Py-Ind (**5**) and compared them with those of β-D-Xyl-Py-γ-Py-Ind (**4**). Interestingly, the replacement of the β-linkage by an α-linkage changes the electronic properties of the indole chromophore. The quantum yield value for the α-anomer is slightly higher than that for the β-anomer (see Table 1 and Figure 1).

This difference is in agreement with the different conformation of the sugar in relation to the oligoamide fragment predicted by molecular modelling. The β-anomer, in which

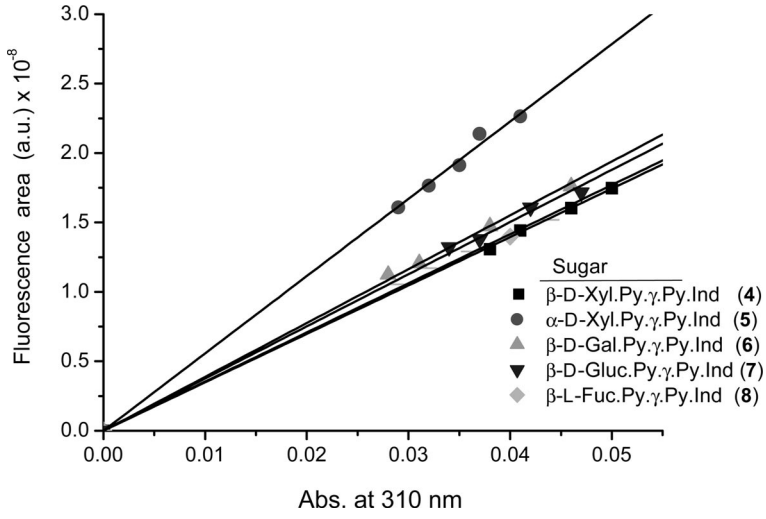

Figure 1. Linear plot for ligands **4**–**8** of integrated fluorescence intensity vs. absorbance, calculated in phosphate buffer (λ_{exc} = 310 nm, pH 7.3).

the sugar is placed in the vicinity of the indole ring, quenched the fluorescence emission slightly more than the α-anomer, in which the sugar is placed out of the plain of the oligoamide in the hairpin structure[49] (see Figure S3 in the Supporting Information).

We also determined the fluorescence quantum yields of the vector-oligoamides **1**, **2** and **3** and compared them with those of sugar-oligoamide **4** and with the indole-strand model **10**. Since **1** and **3** are not soluble in phosphate buffer solution, we used DMSO (7% *v*/*v*) as co-solvent for all the measurements. The values are given in Table 2.[65]

Table 2. Fluorescence quantum yields for ligand **4**, vectors **1**–**3** and models **9**–**10** measured in buffer solution containing 7% (v/v) DMSO.

Ligands		$\Phi_f \times 10^{-3}$
MeNH-Py-γ-Py-Ind	**1**	16.32
MeO-Py-γ-Py-Ind	**2**	25.31
Cycl-Py-γ-Py-Ind	**3**	28.16
β-Xyl-Py-γ-Py-Ind	**4**	3.81
β-Xyl-Py-NHAc	**9**	1.37[a]
(EtO)-γ-Py-Ind	**10**	47.13

[a] Not indole but pyrrole fluorophore.

These new experimental conditions did not significantly alter the Φ values of β-D-Xyl-Py-γ-Py-Ind (**4**), β-D-Xyl-Py-NHAc (**9**) and (EtO)-γ-Py-Ind (**10**) relative to buffer (see Table 1 and Table 2).

Again, **10** shows a very high quantum yield in relation to sugar-oligoamide **4**, suggesting intramolecular quenching of the indole fluorophore in the hairpin structure. With regard to the aliphatic vector-oligoamides **1**, **2** and **3**, all present quantum yield values greater than that of **4**, but smaller than that of the indole strand model **10** with an extended conformation (Figure 2).

The unexpected higher values of quantum yields of **1**–**3** relative to **4** can be explained by taking two different factors into account:

a) C–H–π interactions should be more effective in carbohydrates than in alkanes since C–H systems adjacent to OH groups are more acidic than aliphatic C–H systems. Thus, in the case of the sugar-oligoamide **4** the hairpin structure should be stabilized not only by π–π interaction of the pyrrole rings in both strands but also by sugar C–H–π interaction, producing more effective indole fluorescence quenching.

b) There are differences in the effect of C–H (aliphatic) and C–OH (or C–H acidic) groups in the quenching of the indole fluorophore that are intrinsic to the natures of the different groups (OH groups being more effective quenchers than CH groups).[66]

We believe that in an aqueous solution the contribution of this second factor (the chemical nature of the residue above the indole) should be less important. Nevertheless, the Φ_f values of Cycl **3** (apolar) and β-D-Xyl **4** (polar) with similar steric demand cannot be completely correlated with differences in the stabilities of their hairpin structures in solution (Table 2).

With regard to the difference between the methyl amide and the cyclohexyl amide, with their virtually identical chemical natures, we also believe the methyl group allows closer proximity between the two strands in the hairpin conformation, thus favouring the fluorescence quenching, and that the Φ_f value for Me **1** should then be lower than that for the Cycl **3**.

To support the fluorescence data, we also studied the conformations of the vectors **1**–**3** in aqueous solution by NMR spectroscopy. Full assignment of the ^{1}H NMR spectra of **1**–**3** was carried out by COSY and NOESY experiments in H_2O/[D_6]acetone (1:1) mixtures.[67] A comparative study of the chemical shifts of proton resonances of **1**–**3**

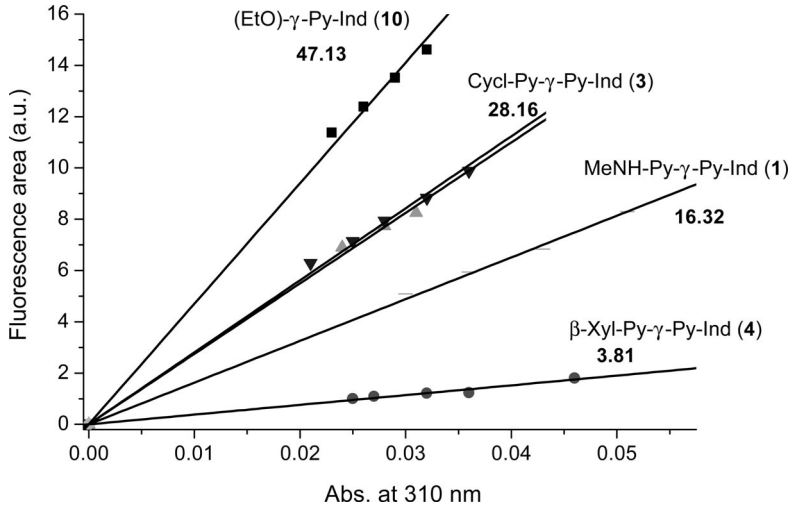

Figure 2. Linear plot of integrated fluorescence intensity vs. absorbance for ligands **1**, **3**, **4** and **10**, calculated in phosphate buffer/7% (v/v) DMSO (λ_{exc} = 310 nm, pH 7.3).

with the indole-strand EtO-γ-Py-Ind (**10**) and Cycl-Py-NHAc model shows chemically induced shifts (CISs) in **1**–**3** compatible with the presence of certain percentages of hairpin conformations in solution.

In the case of the new ligands described here, shielding effects in the pyrrole resonances (P^{3A}, P^{3B}, P^{5A} and P^{5B}) of up to 0.21 ppm was found (see Table S3, Supporting Information), in the same range as the CIS values previously described for sugar-oligoamides **4**, **6** and **7** (CISs in the pyrrole resonances of up to 0.15 ppm were found for sugar-oligoamides **4**, **6** and **7** in D_2O/[D_6]acetone and up to 0.28 ppm in D_2O solution).[49] Unfortunately, the vector-oligoamides **1**–**3** could not be studied under the same conditions, due to solubility problems.

Moreover, Figure 3 shows the inter-strand nOes that give further evidence of the presence of certain percentages of hairpin conformations in aqueous solution in the cases of vectors **1**–**2** (see Table S2 in the Supporting Information).[68]

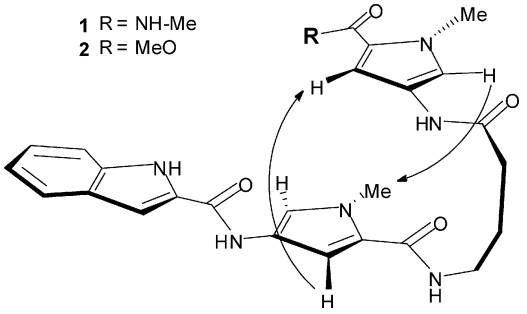

Figure 3. Inter-strand nOes found in the ROESY spectra of vector-oligoamides **1**–**2** in D_2O/[D_6]acetone (1:1) at 26 °C.

Additionally, the NOESY experiment in H_2O for Cycl **3** shows cross peaks from the NH of the indole ring resonance with two proton resonances of the cyclohexyl as shown in Figure 4.

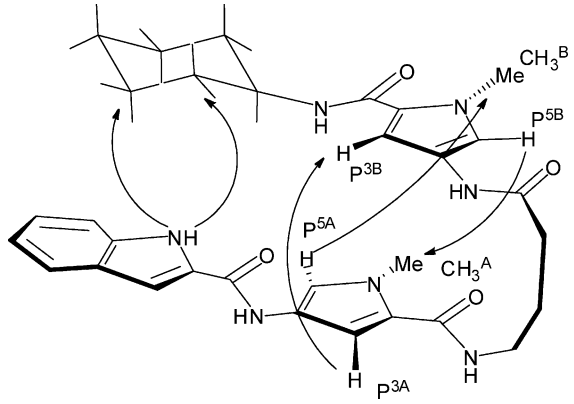

Figure 4. Inter-strand nOes found in a NOESY experiment with Cycl **3** (T = 26 °C) in H_2O.

The fluorescence and NMR structural data thus also support the presence of certain percentages of hairpin structure in solution in the vector ligands **1**–**3**.

Binding Studies of Vector-Oligoamides 1–3 and Sugar-Oligoamides 4–8 with *ct*-DNA, *ml*-DNA and *poly*(dA-dT)

As a first step, we carried out a quantitative study of the binding of the neutral vector-oligoamides **1**–**3** to *ct*-DNA (60% AT, 40% GC), *poly*(dA-dT) (100% AT) and *ml*-DNA (72%GC, 28% AT) in order to test whether the designed oligoamide structure (-Py-γ-Py-Ind) can be used as DNA-sequence-selective carrier (see Supporting Information). Moreover, in order to explore the minimum oligoamide structure of the carrier, the binding of the sugar strand **9** and the indole strand **10** were also studied.

We initiated our fluorescence binding studies by examining the characteristics of a solution of the vector-oligoamide **1** titrated with a concentrated solution of *ct*-DNA.

An enhancement in fluorescence emission was observed (see Figure S4 in the Supporting Information).[21,69]

To confirm that the fluorescence enhancement observed upon addition of *ct*-DNA was a result of the binding of the vector-oligoamide to *ct*-DNA, a series of control experiment were carried out (see Figures S5–S7 in the Supporting Information). In addition, β-D-Xyl-Py-NHAc (**9**) and (EtO)-γ-Py-Ind (**10**) were titrated independently with the same concentrated stock solution of *ct*-DNA under the same experimental conditions as described for **1**. During the addition of *ct*-DNA, a linear decrease in fluorescence emission was observed, consistent with the expected ligand dilution. A titration experiment in which both β-D-Xyl-Py-NHAc (**9**) and (EtO)-γ-Py-Ind (**10**) were present at the same concentration was then carried out, and again a decrease in fluorescence was observed. All these pieces of evidence indicate that neither these isolated fragments (indole-strand and the sugar-strand) nor the 1:1 mixture are DNA binders (see Figures S8–S9 in the Supporting Information).

The non-carbohydrate-oligoamide models **1** and **3** were then titrated with *ct*-DNA. In both cases, significant increases in fluorescence emission as the addition of DNA was taking place were found. The increase in fluorescence intensity with increasing addition of DNA showed a binding isotherm profile that was fitted to a 1:1 binding model with Specfit/32® (Spectrum Software Associates) (see Figures S10 and S11 in the Supporting Information).

The K_a values obtained by nonlinear regression and the calculated $\Delta G°$ values are given in Table 3. The K_a values are in the 10^4 M^{-1} range for both derivatives, the complex with Cycl **3** being slightly more stable than the one with Me **1** [$\Delta\Delta G°$ (**3** –**1**) = –0.4 kcal mol^{-1}].

The same fluorescence binding experiments were then carried out with *ml*-DNA. This polymer was selected in order to explore the effect on the K_a value of increasing the GC base pair concentration. The K_a values of the complexes formed by **1** and **3** vectors with *ml*-DNA (see Table 3 and Figure 5) did not change a lot with respect to *ct*-DNA (10^4 M^{-1} range).

We thus explored complexation with *poly*(dA-dT). The saturation point of the binding isotherm was achieved at a very early stage of *poly*(dA-dT) addition (ca. 1 μM) under these experimental conditions, suggesting very efficient binding. The calculated K_a values are in the 10^6 to 10^7 M^{-1} range (Table 3). Significantly, the K_a values are two or three orders of magnitude higher than those measured for *ct*-DNA and *ml*-DNA ($\Delta\Delta G°$ (*poly*(dA-dT) – (*ct*-DNA) = –(2.5–3.8) kcal mol^{-1}), which confirms that the vector ligands **1** and **3** are selective for –(AT)$_n$– sequences.[51]

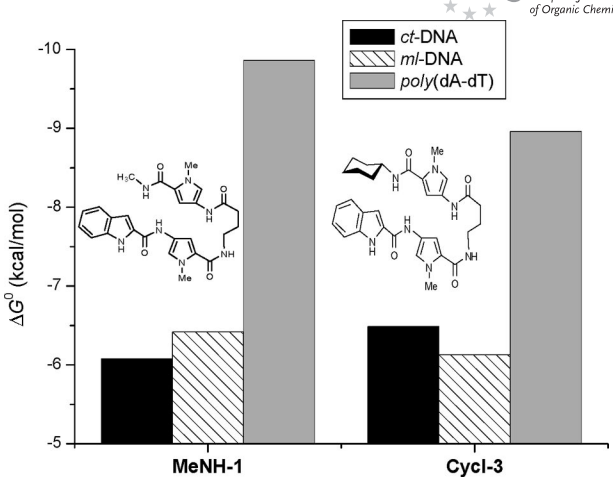

Figure 5. Binding constants calculated for the vector derivatives Me **1** and Cycl **3** with the polymeric DNA models *ct*-DNA, *ml*-DNA and poly(dA-dT).

Comparison of the K_a values for **1** and **3** complexes with *poly*(dA-dT) showed that the Me compound **1** is more stable than the one with the Cycl **3** at the C-terminus [$\Delta\Delta G°$ (**1**–**3**) = –0.9 kcal mol^{-1}], which is in agreement with results previously reported by Dervan, which suggest that a bulky group at the C terminus of a larger synthetic oligoamide destabilizes the interaction.[16]

With regard to compound MeO-Py-γ-Py-Ind (**2**), which has the oligoamide structure except that the amide residue at the C terminus has been replaced by an ester linkage, no binding to DNA was detected with any of the DNA models at any ligand or DNA concentrations allowed in the fluorescence experiment[70] (see Figure S12 in the Supporting Information).

These results indicate that the C-terminal amide residue is essential for our short oligoamide fragment to act as an effective DNA minor groove ligand and that -Py-γ-Py-Ind is the *minimum oligoamide structure* of the (–ATAT–)-selective carrier.

Moreover, these carriers **1**, **3** possess binding constants and selectivities (Table 3 and Figure 5) in the same range as those of other structurally related synthetic charged oligoamides such as Im-Py-*Py*-γ-*Py*-Py-Py-Dp, which are

Table 3. Binding constants calculated for the vector derivatives Me **1** and Cycl **3** with the polymeric DNA models *ct*-DNA, *ml*-DNA and *poly*(dA-dT).

		MeNH **1**	Cycl **3**
ct-DNA	K_a (M^{-1})	$2.9 \times 10^4 \pm 6.12 \times 10^3$	$5.75 \times 10^4 \pm 1.34 \times 10^4$
	$\Delta G°$ (kcal mol^{-1})	–6.08 ± 0.13	–6.49 ± 0.14
ml-DNA	K_a (M^{-1})	$5.08 \times 10^4 \pm 2.03 \times 10^4$	$3.12 \times 10^4 \pm 1.39 \times 10^4$
	$\Delta G°$ (kcal mol^{-1})	–6.42 ± 0.25	–6.13 ± 0.28
poly(dA-dT)	K_a (M^{-1})	$1.70 \times 10^7 \pm 4.71 \times 10^6$	$3.72 \times 10^6 \pm 5.84 \times 10^5$
	$\Delta G°$ (kcal mol^{-1})	–9.86 ± 0.17	–8.96 ± 0.09

larger than ours.[15,71] We can thus conclude that our vector is the smallest fragment necessary in order to show efficient and selective (–ATAT–)-binding to DNA.

The next step in our investigation was to study the binding characteristic of the sugar oligoamides **4**–**8** in order to check whether the affinity and selectivity shown by the vector ligands remained when a saccharide fragment was placed at the C terminus of such a vector. Additionally, quantitative access to the role of the carbohydrate in complexation could be extracted from this set of data.

With regard to binding to *ct*-DNA, the K_a values for all the derivatives are in the 10^4 M^{-1} range, the most stable complex being that of β-Xyl **4** ($K_a = 3.24 \times 10^5$ M^{-1}) and the weakest one that of α-Xyl **5** ($K_a = 1.07 \times 10^4$ M^{-1}). This difference reflects the conjecture that the carbohydrate plays a role in complexation (see Table 4).

Table 4. Binding constants and $\Delta G°$ values calculated for the ligand (**1**, **3**–**8**)/*ct*-DNA complexes.

ct-DNA Ligands	K_a (M^{-1})	$\Delta G°$ (kcal mol^{-1})
1	$2.90 \times 10^4 \pm 6.12 \times 10^3$	–6.08 ± 0.13
3	$5.75 \times 10^4 \pm 1.34 \times 10^4$	–6.49 ± 0.14
4	$3.24 \times 10^5 \pm 9.27 \times 10^4$	–7.51 ± 0.17
5	$1.07 \times 10^4 \pm 2.16 \times 10^3$	–5.49 ± 0.12
6	$7.08 \times 10^4 \pm 1.49 \times 10^4$	–6.61 ± 0.13
7	$2.94 \times 10^4 \pm 4.23 \times 10^3$	–6.09 ± 0.09
8	$1.95 \times 10^4 \pm 5.18 \times 10^3$	–5.85 ± 0.16

Comparison of the K_a values of the complex of vector **3** with those of the sugar oligoamides **4**–**8** shows that some sugar derivatives **4**, **6** exhibit an increase in the binding in comparison with **3**, with the highest stabilization being shown by compound **4** [$\Delta\Delta G°$ (**4** – **3**) = –1.0 kcal mol^{-1}] (see Table 4). However, other sugar derivatives **5**, **7**–**8** show decreases in stability, **5** being the least stable [$\Delta\Delta G°$ (**5** – **3**) = +1.0 kcal mol^{-1}].

With regard to the difference in configuration produced by α or β linkage of the sugar ring to the oligoamide, the change in orientation of the sugar in the general structure of the hairpin gives rise to significant differences in binding, the β-D-Xyl **4** complex being more stable than the α-D-Xyl **5** one [$\Delta\Delta G°$ (**4** – **5**) = –2.0 kcal mol^{-1}].

The K_a values of the complexes formed by the sugar-oligoamides **4**–**8** with *ml*-DNA did not change a lot with respect to *ct*-DNA (10^4 M^{-1} range), as expected (see Table 5).

In this case, β-L-Fuc **8**:*ml*-DNA is the most stable complex, while α-D-Xyl **5**:*ml*-DNA is again the least stable one [$\Delta\Delta G°$ (**8** – **5**) = –1.1 kcal mol^{-1}].

The binding difference between the complexes formed both by α-D-Xyl and by β-D-Xyl ligands in terms of $\Delta G°$ is [$\Delta\Delta G°$ (**4** – **5**) = –1.0 kcal mol^{-1}]. Again, the β-D-Xyl complex **4** is more stable than the α-D-Xyl one **5**.

Additionally, all sugar-oligoamides complexes are more stable than those measured for the vector Cycl **3** (except for α-D-Xyl **5**, which is about 0.4 kcal mol^{-1} less stable than **3**; see Table 5).

Table 5. Binding constants and $\Delta G°$ values calculated for the ligand (**1**, **3**–**8**)/*ml*-DNA complexes.

ml-DNA Ligands	K_a (M^{-1})	$\Delta G°$ (kcal mol^{-1})
1	$5.08 \times 10^4 \pm 2.03 \times 10^4$	–6.42 ± 0.25
3	$3.12 \times 10^4 \pm 1.39 \times 10^4$	–6.13 ± 0.28
4	$7.83 \times 10^4 \pm 2.76 \times 10^4$	–6.67 ± 0.22
5	$1.51 \times 10^4 \pm 6.08 \times 10^3$	–5.70 ± 0.25
6	$4.27 \times 10^4 \pm 2.82 \times 10^4$	–6.31 ± 0.47
7	$1.00 \times 10^5 \pm 5.42 \times 10^4$	–6.82 ± 0.36
8	$9.55 \times 10^4 \pm 3.02 \times 10^4$	–6.79 ± 0.19

Furthermore, K_a values of complexes of sugar-oligoamides **4**–**8** with *poly*(dA-dT) were also measured under the same experimental conditions as in the case of the vector models **1**–**3** (see Table 6).

Table 6. Binding constants and $\Delta G°$ values calculated for the ligand (**1**, **3**–**8**)/*poly*(dA-dT) complexes.

poly(dA-dT) Ligands	K_a (M^{-1})	ΔG^0 (kcal mol^{-1})
1	$1.70 \times 10^7 \pm 4.71 \times 10^6$	–9.86 ± 0.17
3	$3.72 \times 10^6 \pm 5.84 \times 10^5$	–8.96 ± 0.09
4	$3.72 \times 10^6 \pm 4.63 \times 10^5$	–8.96 ± 0.08
5	$4.93 \times 10^6 \pm 5.03 \times 10^5$	–9.13 ± 0.06
6	$5.95 \times 10^7 \pm 1.68 \times 10^7$	–10.6 ± 0.17
7	$1.20 \times 10^7 \pm 1.68 \times 10^6$	–9.65 ± 0.08
8	$6.76 \times 10^6 \pm 2.35 \times 10^6$	–9.31 ± 0.21

The interaction of the sugar-oligoamides with this specific polymeric sequence $(AT)_n$ is between two and three orders of magnitude stronger in terms of K_a than those for *ml*-DNA complexes (see Table 6), thus confirming that the general structure (sugar-Py-γ-Py-Ind) could be used for the production of carbohydrate DNA carriers selective for –ATAT– sequences {$\Delta\Delta G°$ [*poly*(dA-dT) – *ml*-DNA] = –(2.3–4.3) kcal mol^{-1}}. All sugar-oligoamide complexes other than those of β-D-Xyl **4** are more stable than those of the vector Cycl **3**. Hence, the sugar that gives the most stable complex is β-D-Gal **6** [$\Delta\Delta G°$ (**6** – **3**) = –1.7 kcal mol^{-1}].

Comparison between $\Delta G°$ values of the different ligand complexes with *poly*(dA-dT) shows that there is 1.7 kcal mol^{-1} difference between the most stable β-D-Gal **6**/*poly*(dA-dT) and the least stable β-D-Xyl **4**/*poly*(dA-dT) complexes.[72]

This particular DNA sequence gives complexes with quite similar binding for α- and β-D-Xyl-oligoamide complexes [$\Delta\Delta G°$ (**5** – **4**) < –0.2 kcal mol^{-1}].

It is highly remarkable that β-D-Gal **6** shows some of the weakest binding with *ml*-DNA (which presents the smallest percentage of AT sequence) while it gives the strongest binding with *poly*(dA-dT). Thus, β-D-Gal **6** is the most sequence-selective sugar-oligoamide {$\Delta\Delta G°$ **6** [*poly*(dA-dT)–*ml*-DNA] = –4.3 kcal mol^{-1}}.

We thus decided to measure the binding affinity of β-D-Gal **6** with *poly*(dC-dG) [100% of $(CG)_n$ sequences].

The value (K_a = 4.55 × 10^3 M^{-1}, $\Delta G°$ = –4.99 kcal mol^{-1}) is smaller than that measured for β-D-Gal-Py-γ-Py-Ind (**6**) with *ml*-DNA [72% of $(CG)_n$ sequences], as expected {$\Delta\Delta G°$ β-D-Gal **6** [*ml*-DNA – *poly*(dC-dG)] = –1.3 kcal mol^{-1}}, and more relevantly, the AT/CG selectivity is $\Delta\Delta G°$ β-D-Gal **6** [*poly*(dA-dT) – *poly*(dC-dG)] = –5.6 kcal mol^{-1}.

All the collected binding experiments confirm that the vector is a carbohydrate –ATAT–carrier exhibiting a selectivity of around 3 kcal mol^{-1} and, more remarkably, that the carbohydrate also plays a role in this sequence selectivity, the β-D-Gal **6** being the most –ATAT– selective sugar-oligoamide for this particular sequence and β-D-Xyl **4** the least selective one.

Now we can also conclude that our neutral oligoamides clearly bind preferentially to AT-rich DNA sequences. The selectivity found is even higher than that observed, under similar experimental conditions, for the naturally occurring polyamide antibiotic netropsin {$\Delta\Delta G°$ [*poly*(dA-dT) – *ct*-DNA] = –2.3 kcal mol^{-1}}[73,74] and for other minor groove binders such as Hoechst-33258 {$\Delta\Delta G°$ [*poly*(dA-dT) – *ct*-DNA] = –1.0 kcal mol^{-1}}[14] and DAPI {$\Delta\Delta G°$ [*poly*(dA-dT) – *ct*-DNA] = –0.4 kcal mol^{-1}},[75] all of them being charged ligands,[76] even though the binding constants of these charged compounds are higher, as would be expected.

Finally, binding studies of our sugar-oligoamides with a short and defined oligonucleotide sequence were carried out in order to confirm that the vector (-Py-γ-Py-Ind) can transport a monosaccharide to a unique binding site in a selective manner.

We chose the Drew–Dickerson dodecamer:[77–79] d(CGCGAATTCGCG)$_2$ in which the AT sequence is present.[80]

Sugar-oligoamide β-D-Xyl-Py-γ-Py-Ind (**4**) was chosen as the least selective of all our molecules towards AT/TA sequences, thus evaluating the most unfavourable situation regarding poly-binding phenomena. Binding titrations were carried out by the same procedure as in the case of polymeric DNAs.

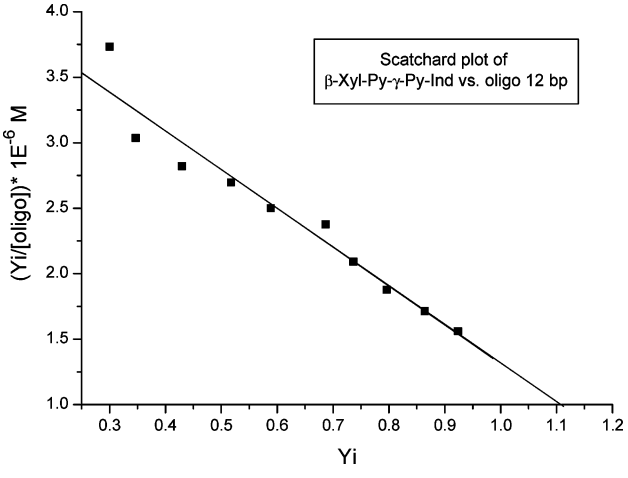

Figure 6. Scatchard plot of β-D-Xyl-Py-γ-Py-Ind (**4**) with the Drew-Dickerson dodecamer.

The 1:1 stoichiometry of the sugar-oligoamide–oligonucleotide complexes was confirmed both by a Scatchard plot and by Job[59] experiments with β-D-Xyl-Py-γ-Py-Ind (**4**) and the Drew–Dickerson dodecamer (see Figure 6 and Figure 7) and the binding constants for an expected 1:1 complex were calculated. The observed K_a values confirmed that the affinity of our ligand for short oligonucleotide sequences is in the same range as measured in the case of polymeric DNA models: K_a β-D-Xyl **4** vs. d(CGCGAATTCGCG)$_2$ = 1.78 × 10^6 M^{-1}, K_a β-D-Xyl **4** vs. *poly*(dA-dT) = 3.72 × 10^6 M^{-1}.

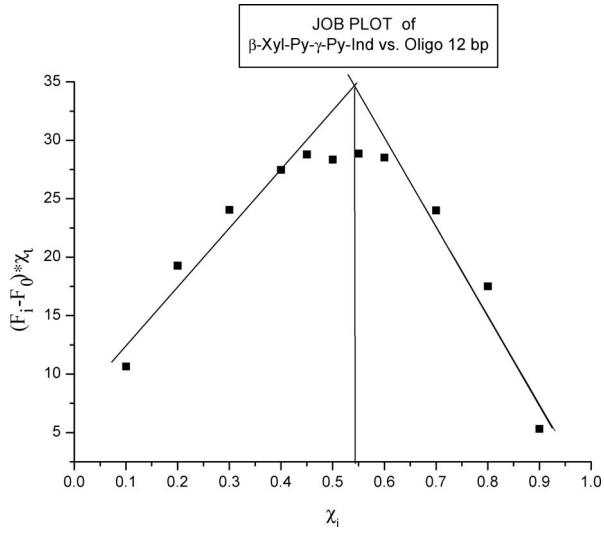

Figure 7. Job experiment with β-D-Xyl-Py-γ-Py-Ind (**4**) and the Drew–Dickerson dodecamer.

Such results from the use of the general structures of our sugar-oligoamides **4**–**8** for systematic binding studies with short DNA sequences allow us insight into the molecular basis of the carbohydrate–DNA interaction.

Conclusions

The binding of distamycin-type γ-linked covalent dimer neutral ligands **1**–**8** to DNA has been quantified. The study has shown that -Py-γ-Py-Ind is the minimum vector-oligoamide fragment that leads to efficient binding, the amide NH at the C terminus of the oligoamide being fundamental to the interaction.

The general structure of the vector provides binding selectivity towards –ATAT– sequences. Additionally, -Py-γ-Py-Ind is a *neutral vector* that can transport sugars to the minor groove in a selective manner since the complexes of **4**–**8** with *poly*(dA-dT) are up to three orders of magnitude more stable that those with *poly*(dC-dG).

The quantification of such selectivity has allowed us to ensure that the sugar-oligoamide ligand designed *allows the monosaccharide to play a role in complexation*. Moreover, the selectivity found is even better than those measured for the charged minor groove ligands Hoechst-33258, netropsin and DAPI.

Finally, we have opened a pathway for use of the general structure of our sugar-oligoamides **4**–**8** for systematic binding studies with short DNA sequences. This should allow us to gain insights into the molecular basis of the carbohydrate–DNA interaction for further rational design of novel glyco-compounds such as antibiotics, anticancer drugs or glycoproteins.

Experimental Section

General: The synthesis of glyco-oligoamides **4**, **6** and **7** and models **9**–**10** was described previously.[49] Ligands **5**, **8** and vectors **1**–**3** were prepared and characterized by the same procedure.

Calf thymus DNA (*ct*-DNA), *poly*(dA-dT) and *ml*-DNA were provided by Sigma–Aldrich and used without further purification. The studied oligonucleotide (HPLC grade) was provided by Isogen (www.isogen.com) and used with no additional purification.

All the spectroscopic measurements (UV as well as fluorescence) were made at room temperature under air saturation conditions in sodium phosphate buffer solution (10 mM) or in the phosphate buffer/7% DMSO mixture (pH 7.3). The 0.2 μm nylon filters were provided by Symta. The water was purified with a Milli-Q system. Analytic grade DMSO was provided by Merck and used without further purification.

The phosphate buffer solution (10 mM) was prepared as follows: two concentrated stock solutions of the monobasic and dibasic salts of sodium phosphate were prepared (A and B, respectively).

Solution A: monobasic sodium phosphate solution (0.2 M, 27.8 g in 1000 mL of distilled water). Solution B: dibasic sodium phosphate solution (0.2 M, 53.65 g of $Na_2HPO_4{\cdot}7H_2O$ in 1000 mL of distilled water). The 10 mM phosphate buffer solution (pH 7.3) is then obtained by mixing A (3.9 mL) and B (6.1 mL) and diluting to a final volume of 200 mL with distilled water. This buffer solution must be prepared every week to avoid deterioration problems.

The UV absorption spectra of the samples were recorded with a double beam Perkin–Elmer Lambda 35 UV/Vis spectrophotometer, with standard 10 mm path length cuvettes. The interval of measured wavelengths is between 200–400 nm. To all the cases the scanning speed was fixed to 240 nm min^{-1} and the width of the slits to 2 nm.

Steady-state fluorescence measurements were made with both Perkin–Elmer LS-50B and Fluorolog-3 (Jobin Yvon-Spex Instruments S.A., Inc., New Jersey) spectrophotometers, for experimental titration and for fluorescence quantum yields determination, respectively. Standard 10 mm path length fluorescence cuvettes were used in these studies. The excitation and emission slits were set at 10 nm, and both excitation and emission were scanned at 20 nm intervals at 300 nm min^{-1}. The refractive index of phosphate buffer solution containing DMSO (7%) was determined at room temperature with an ABBE refractometer (Zeiss) and sodium vapour lamp monochromatic light at 589 nm. NMR measurements were recorded on a Varian Inova 300 (300 MHz), a Varian Inova 400 (400 MHz) and a Varian Unity 500 (500 MHz).

Fluorimetric Characterization of Ligands 1–10: For characterization of the fluorescence properties of ligands **1**–**10**, Me-Py-γ-Py-Ind (**1**) was used. β-D-Xyl-Py-NHAc (**9**) and (EtO)-γ-Py-Ind (**10**) were used as comparison models of their emission and excitation spectra with those of the vector-oligoamide **1**. Ligand solutions were freshly prepared and stirred for one to two hours and filtered through a 0.2 μm nylon filter before the spectra were recorded. The concentrations of the ligands were determined optically by using the molar extinction coefficient (ε; see Table S1, Supporting Information). Emission and excitation spectra for each compound were registered at various emission (from 260 to 355 nm) and excitation wavelengths (from 340 to 380 nm), depending on the experiment (see Figures S1 and S2 in the Supporting Information).

Determination of Molar Extinction Coefficients (ε): Molar extinction coefficients for compounds **1**–**10** were calculated both in the phosphate buffer solution and in the phosphate buffer/7% DMSO mixture, according to the Lambert–Beer law. In the phosphate buffer/7% DMSO mixture the molar extinction coefficients of compounds (**1**–**10**) were calculated as follows: a known amount of ligand (ca. 1.5 mg) was dissolved in DMSO (10 mL). An aliquot (25–250 μL) of that concentrated stock solution was then diluted to 2.8 mL with phosphate buffer solution (the DMSO percentage was set to 7% *v*/*v*). All the values calculated are summarized in Table S1 (Supporting Information).

Fluorescence Quantum Yield (Φ_f) Measurements: Fluorescence quantum yield determinations for compounds **5**–**8** were performed in phosphate buffer solution (η = 1.332), compounds **1**–**3** were measured in phosphate buffer/7% DMSO mixture (η = 1.343), while compounds **4**, **9** and **10** were measured in both solvents for reasons of comparison.

For both solvents, quantum yields (Φ) were measured relative to a standard that emits in a region close to our test samples (λ_{em} = 350 nm). Of the available standard compounds, quinine bisulfate in H_2SO_4 (0.1 M, Φ = 0.546) was selected.[81,82]

Absorbance of the measured test samples and standard solutions did not exceed 0.05, to avoid reabsorption of the emitted fluorescence.[83] Solutions were prepared with different absorbances, ranging from 0.02 to 0.05. UV absorbance at the excitation wavelength (310 nm) and fluorescence emission spectra of a series of solutions of the standard and compounds **1**–**10** were recorded.

The final fluorescence spectra were derived by subtraction of the solvent spectrum from the sample spectra. The areas of the resulting fluorescence emission spectra were then calculated by use of the Origin 6.0 program and they were plotted vs. the absorbance. Linear plots with a zero intercepts were obtained and their gradients (Grad) were determined.

The gradient for each sample is proportional to that sample's fluorescence quantum yield. Absolute values were calculated with the aid of the standard sample, which has a fixed and known fluorescence quantum yield value, according to the following Equation (1).

$$\Phi_x = \Phi_{st}\left(\frac{Grad_x}{Grad_{st}}\right)\left(\frac{\eta_x^2}{\eta_{st}^2}\right) \quad (1)$$

The subscripts st and x denote standard and test, respectively. The value Φ is the fluorescence quantum yield, *Grad* is the gradient from the plot of integrated fluorescence intensity vs. absorbance, and η is the refractive index of the solvent. Tables 2 and 3 summarize the Φ_f values for ligands **1**–**10**.

Structural Studies. ^{1}H NMR Experiments: All the spectra in aqueous solution were recorded with presaturation of the water signal. The chemical shifts were reported in ppm relative to residual acetone (δ = 2.04 ppm) when D_2O/[D_6]acetone or H_2O/[D_6]acetone was used in the experiment. NMR structural studies of compounds

1–**3** were based on monodimensional and bidimensional (COSY, HSQC, HMBC, ROESY) experiments and were recorded at 400 or 500 MHz and 26 °C in a Varian instrument. Sample solutions were prepared at concentrations ranging between 2 and 0.1 mM, depending on the solubility of the compounds.

Dilution Experiments: Dilution experiments with compounds **1**–**3** were carried out in D_2O/[D_6]acetone at 26 °C. Concentrations of the vector-oligoamides ranged between 2 mM and 0.09 mM in D_2O/[D_6]acetone. Compounds **1**–**3** do not auto-associate under the experimental conditions used.

Binding Studies. General Procedure for Determination of Binding Constants (K_a) between Ligands 1–8 and DNA by Fluorescence Spectroscopy: The ligand solution was freshly prepared by dissolving the compound in phosphate buffer solution containing DMSO (7% *v*/*v*). The mixture was stirred for one to two hours and was then filtered through a 0.2 μm nylon filter. The concentration of the ligand was determined optically by use of their molar extinction coefficients (Table S1, Supporting Information). The percentage of DMSO was kept constant at 7% during the titration experiment.

The DNA concentration in base pairs was determined by UV/Vis. absorption spectroscopy by use of extinction coefficients of 13200 M^{-1} cm^{-1} at 260 nm for *ct*-DNA, *poly*(dA-dT) and *ml*-DNA according to the literature.[84,85] Solid *ct*-DNA (2 mg) was dissolved in 1 mL, *poly*(dA-dT) in 1 mL and *ml*-DNA in 4.5 mL of phosphate buffer/7% DMSO mixture (in this last case, the DNA had to be shaken 30 minutes at 37 °C and sonicated for 5 min in an ultrasound bath, due to DNA solubility problems).

Spectrofluorimetric titrations were carried out by titrating the sugar-oligoamide solution with a concentrated solution of *ct*-DNA (2.51×10^{-3} M), *poly*(dA-dT) (2.5×10^{-5} M), *ml*-DNA (1.1×10^{-3} M) or *poly*(dC-dG) (3.49×10^{-3} M).

The ligand sample has to be shaken vigorously for at least 30 minutes until fluorescence emission spectra stabilization before DNA addition.

The emission and excitation slits were both fitted to 10, the scan speed was 300 nm min^{-1}, and the initial volume of ligand/model solutions in the fluorescence cuvettes was 2.8 mL.

After each DNA addition the sample was also vigorously shaken and the data were recorded after fluorescence emission was stable. An enhancement of the emitted fluorescence (in arbitrary units) was observed after each addition. This enhancement in the emission fluorescence spectra means a variation of the signal from 25 to 300% (depending on the experiment).

A control sample solution of identical concentration was prepared and measured during the experiment to rule out enhancement of the emitted fluorescence due to slow solubilization of the sample (see Figures S5–S7, Supporting Information).

The fluorescence emission spectra were registered and the values of the emission maxima were collected and plotted vs. the DNA total concentration. The experimental data were fitted to a 1:1 binding model by use of the programme Specfit/32® (Spectrum Software Associates) (see Figures S10–S11 in the Supporting Information).

The concentration range of ligand and DNA were fixed to define the binding isotherm (20–80% saturation). Each titration experiment was repeated al least twice, and the K_a values (M^{-1} in base pairs) summarized in Tables 4 to 6 are the averages of all the values measured.

Gibbs free energy values were obtained from the macroscopic binding constants previously calculated according to the equation: $\Delta G° = -RT\mathrm{Ln}K_a$, R being the universal gas constant (1.986×10^{-3} kcal K^{-1} mol^{-1}) and T the ligand solution temperature expressed in Kelvin (298 K).

Fluorescence Titration Experiments of Models 1–3 and Ligands 4–8 with *ct*-DNA: The *ct*-DNA concentration (ca. 2.51×10^{-3} M in base pairs) and the model and/or ligand concentrations (1×10^{-6} to 1×10^{-7} M) were determined by absorption spectroscopy by use of their extinction coefficients.

The excitation wavelength was in all cases fitted to 310 nm, where DNA does not interfere with the fluorescence. The emission wavelengths were fitted depending on the corresponding values for each molecule (see Table S1, Supporting Information).

A K_a value could be measured in each case, except for that of the model MeO-Py-γ-Py-Ind (**2**), which was titrated at different vector concentrations (from 1×10^{-6} M to 5×10^{-8} M) and DNA concentrations [from 1×10^{-4} M to 3.2×10^{-3} M for *ct*-DNA, from 5×10^{-6} M to 2×10^{-5} M for *poly*(dA-dT) and at 1×10^{-3} M for *ml*-DNA] (Figure S12 in the Supporting Information).

Fluorescence Titration Experiments of Models 1–3 and Ligands 4–8 with *ml*-DNA: The concentration of the ligand or model was fitted to 10^{-6} to 10^{-7} M, and the *ml*-DNA concentration in base pairs was found to be ca. 1.1×10^{-3} M. The excitation wavelength was fitted to 310 nm in all cases, and the emission wavelengths were fitted depending on the corresponding values for each molecule (see Table S1, Supporting Information).

Fluorescence Titration Experiments of Models 1–3 and Ligands 4–8 with *poly*(dA-dT): The concentration of the ligand or model was fitted to 10^{-7} to 10^{-8} M and the *poly*(dA-dT) concentration in base pairs was found to be ca. 2.5×10^{-5} M. The excitation wavelength was fitted to 295 nm since no interference in the fluorescence occurs at the DNA concentration range in which the titrations were carried out and the indole fluorophore exhibit its absorption maximum at this wavelength. The emission wavelengths were fitted depending on the corresponding values for each molecule (see Table S1 in the Supporting Information).

Fluorescence Titration Experiments of Models 1–3 and Ligands 4–8 with *poly*(dC-dG): The ligand concentration was fitted in these cases to ca. 10^{-6} M for K_a determination in the best possible range. The *poly*(dC-dG) concentration was determined to be ca. 3.5×10^{-3} M in base pairs and the excitation wavelength was again fitted to 310 nm. The concentration range of ligand and DNA could not be fixed to cover between 20 and 80% saturation (maximum saturation reached ca. 33%), due to solubility problems. Thus, the K_a values measured in those cases were not determined under the best possible conditions.

Fluorescence Titration Experiments of β-D-Xyl-Py-γ-Py-ind (4) with Oligonucleotides: As a first step, the annealing of the oligonucleotide had to be carried out by dissolving the sample in the buffer/7% DMSO mixture, heating it into a water bath at 95–100 °C for two minutes and leaving the bath temperature to drop slowly for at least 3 hours.

The ligand (ca. 10^{-7} M) and oligonucleotide (ca. $2–5 \times 10^{-5}$ M) concentrations were fitted by UV/Vis spectroscopy. In the case of the oligonucleotides, the theoretical molar extinction coefficients calculated on the web page (www.ambion.com/techlib/misc/oligo_calculator.html) were used for the concentration determination.

Supporting Information (see also the footnote on the first page of this article): Fluorescence characterization of the ligands **1**–**10** as

well as NMR characterization of the vectors **1**–**3** in the free state are described. Experimental conditions and examples of binding experiments and fluorescence quantum yield measurements are also included.

Acknowledgments

Financial support for this work was provided by the Ministerio de Educación y Ciencia (MEC) (BQU2003-03550-C03-02 and CTQ2006-10874-C02-02) and a European Research Training Network (RTN) project (HPRN-CT-2002-00190). P. P. is grateful to the Consejo superior de Investigaciones Científicas for an I3P predoctoral fellowship. S. A. thanks RTN and MEC for a Juan de la Cierva postdoctoral contract.

[1] A. Abudaya, P. M. Brown, K. R. Fox, *Nucleic Acids Res.* **1995**, *23*, 3385–3392.
[2] I. Haq, J. E. Ladbury, B. Z. Chowdhry, T. C. Jenkins, J. B. Chaires, *J. Mol. Biol.* **1997**, *271*, 244–257.
[3] S. Neidle, *Nat. Prod. Rep.* **2001**, *18*, 291–309.
[4] P. B. Dervan, *Bioorg. Med. Chem.* **2001**, *9*, 2215–2235.
[5] L. H. Hurley, *Nat. Rev. Cancer* **2002**, *2*, 188–200.
[6] F. X. Han, N. Taulier, T. V. Chalikian, *Biochemistry* **2005**, *44*, 9785–9794.
[7] D. Kahne, *Chem. Biol.* **1995**, *2*, 7–12.
[8] J. W. Trauger, E. E. Baird, P. B. Dervan, *Chem. Biol.* **1996**, *3*, 369–377.
[9] J. B. Chaires, *Curr. Opin. Struct. Biol.* **1998**, *8*, 314–320.
[10] L. Wang, C. Bailly, A. Kumar, D. Ding, M. Bajic, D. W. Boykin, W. D. Wilson, *Proc. Natl. Acad. Sci. USA* **2000**, *97*, 12–16.
[11] P. B. Dervan, A. T. Poulin-Kerstien, E. J. Fechter, B. S. Edelson, *Top. Curr. Chem.* **2005**, *253*, 1–31.
[12] U. Pindur, M. Jansen, T. Lemster, *Curr. Med. Chem.* **2005**, *12*, 2805–2847.
[13] P. B. Dervan, *Science* **1986**, *232*, 464–471.
[14] F. G. Loontiens, P. Regenfuss, A. Zechel, L. Dumortier, R. M. Clegg, *Biochemistry* **1990**, *29*, 9029–9039.
[15] J. Y. Cho, M. E. Parks, P. B. Dervan, *Proc. Natl. Acad. Sci. USA* **1995**, *92*, 10389–10392.
[16] M. E. Parks, E. E. Baird, P. B. Dervan, *J. Am. Chem. Soc.* **1996**, *118*, 6147–6152.
[17] J. W. Trauger, E. E. Baird, P. B. Dervan, *Nature* **1996**, *382*, 559–561.
[18] D. M. Herman, E. E. Baird, P. B. Dervan, *J. Am. Chem. Soc.* **1998**, *120*, 1382–1391.
[19] S. White, J. W. Szewczyk, J. M. Turner, E. E. Baird, P. B. Dervan, *Nature* **1998**, *391*, 468–471.
[20] D. S. Pilch, N. Poklar, E. E. Baird, P. B. Dervan, K. J. Breslauer, *Biochemistry* **1999**, *38*, 2143–2151.
[21] C. E. Bostock-Smith, M. S. Searle, *Nucleic Acids Res.* **1999**, *27*, 1619–1624.
[22] J. M. Gottesfeld, C. Melander, R. K. Suto, H. Raviol, K. Luger, P. B. Dervan, *J. Mol. Biol.* **2001**, *309*, 615–629.
[23] F. Rosu, V. Gabelica, C. Houssier, E. De Pauw, *Nucleic Acids Res.* **2002**, *30*, e82.
[24] M. A. Marques, R. M. Doss, A. R. Urbach, P. B. Dervan, *Helv. Chim. Acta* **2002**, *85*, 4485–4517.
[25] C. A. Briehn, P. Weyermann, P. B. Dervan, *Chem. Eur. J.* **2003**, *9*, 2110–2122.
[26] P. B. Dervan, B. S. Edelson, *Curr. Opin. Struct. Biol.* **2003**, *13*, 284–299.
[27] R. M. Doss, M. A. Marques, S. Foister, P. B. Dervan, *Chem. Biodiversity* **2004**, *1*, 886–899.
[28] S. Walker, K. G. Valentine, D. Kahne, *J. Am. Chem. Soc.* **1990**, *112*, 6428–6429.
[29] D. E. Wemmer, P. B. Dervan, *Curr. Opin. Struct. Biol.* **1997**, *7*, 355–361.
[30] H. Iida, G. F. Jia, J. W. Lown, *Curr. Opin. Biotechnol.* **1999**, *10*, 29–33.
[31] J. Hunziker, *Chimia* **1996**, *50*, 248–256.
[32] C. J. Shelton, M. M. Harding, A. S. Prakash, *Biochemistry* **1996**, *35*, 7974–7982.
[33] R. Katahira, M. Katahira, Y. Yamashita, H. Ogawa, Y. Kyogoku, M. Yoshida, *Nucleic Acids Res.* **1998**, *26*, 744–755.
[34] B. Willis, D. P. Arya, *Curr. Org. Chem.* **2006**, *10*, 663–673.
[35] C. Liu, B. M. Smith, K. Ajito, H. Komatsu, L. Gomez Paloma, T. H. Li, E. A. Theodorakis, K. C. Nicolaou, P. K. Vogt, *Proc. Natl. Acad. Sci. USA* **1996**, *93*, 940–944.
[36] T. H. Li, Z. J. Zeng, V. A. Estevez, K. U. Baldenius, K. C. Nicolaou, G. F. Joyce, *J. Am. Chem. Soc.* **1994**, *116*, 3709–3715.
[37] S. Walker, R. Landovitz, W. D. Ding, G. A. Ellestad, D. Kahne, *Proc. Natl. Acad. Sci. USA* **1992**, *89*, 4608–4612.
[38] K. C. Nicolaou, W. M. Dai, *Angew. Chem. Int. Ed. Engl.* **1991**, *30*, 1387–1416.
[39] L. Wells, K. Vosseller, G. W. Hart, *Science* **2001**, *291*, 2376–2378.
[40] L. Bertram, D. Blacker, K. Mullin, D. Keeney, J. Jones, S. Basu, S. Yhu, M. G. McInnis, R. C. P. Go, K. Vekrellis, D. J. Selkoe, A. J. Saunders, R. E. Tanzi, *Science* **2000**, *290*, 2302.
[41] N. E. Zachara, G. W. Hart, *Chem. Rev.* **2002**, *102*, 431–438.
[42] M. L. de la Paz, J. Jimenez-Barbero, C. Vicent, *Chem. Commun.* **1998**, 465–466.
[43] F. J. Luque, J. M. Lopez, M. L. de la Paz, C. Vicent, M. Orozco, *J. Phys. Chem. A* **1998**, *102*, 6690–6696.
[44] J. Hawley, N. Bampos, N. Aboitiz, J. Jimenez-Barbero, M. L. de la Paz, J. K. M. Sanders, P. Carmona, C. Vicent, *Eur. J. Org. Chem.* **2002**, 1925–1936.
[45] M. L. de la Paz, G. Ellis, M. Perez, J. Perkins, J. Jimenez-Barbero, C. Vicent, *Eur. J. Org. Chem.* **2002**, 840–855.
[46] M. L. de la Paz, C. Gonzalez, C. Vicent, *Chem. Commun.* **2000**, 411–412.
[47] E. M. Munoz, M. L. de la Paz, J. Jimenez-Barbero, G. Ellis, M. Perez, C. Vicent, *Chem. Eur. J.* **2002**, *8*, 1908–1914.
[48] V. Vicente, J. Martin, J. Jimenez-Barbero, J. L. Chiara, C. Vicent, *Chem. Eur. J.* **2004**, *10*, 4240–4251.
[49] J. N. Martin, E. M. Munoz, C. Schwergold, F. Souard, J. L. Asensio, J. Jimenez-Barbero, J. Canada, C. Vicent, *J. Am. Chem. Soc.* **2005**, *127*, 9518–9533.
[50] C. A. Hawkins, R. P. de Clairac, R. N. Dominey, E. E. Baird, S. White, P. B. Dervan, D. E. Wemmer, *J. Am. Chem. Soc.* **2000**, *122*, 5235–5243.
[51] The aromatic amino acid (Py) is known to be AT/TA-selective: S. White, E. E. Baird, P. B. Dervan, *Biochemistry* **1996**, *35*, 12532–12537.
[52] A. R. Urbach, J. W. Szewczyk, S. White, J. M. Turner, E. E. Baird, P. B. Dervan, *J. Am. Chem. Soc.* **1999**, *121*, 11621–11629.
[53] Determined by Wemmer in the bound state for larger oligoamide dimers such as Im-Py-Py-γ-Py-Py-Py-Dp; a) C. A. Hawkins, R. P. de Clairac, R. N. Dominey, E. E. Baird, S. White, P. B. Dervan, D. E. Wemmer, *J. Am. Chem. Soc.* **2000**, *122*, 5235–5243.
[54] M. Mrksich, P. B. Dervan, *J. Am. Chem. Soc.* **1994**, *116*, 3663–3664.
[55] M. Mrksich, M. E. Parks, P. B. Dervan, *J. Am. Chem. Soc.* **1994**, *116*, 7983–7988.
[56] W. A. Greenberg, E. E. Baird, P. B. Dervan, *Chem. Eur. J.* **1998**, *4*, 796–805.
[57] S. White, E. E. Baird, P. B. Dervan, *J. Am. Chem. Soc.* **1997**, *119*, 8756–8765.
[58] V. C. Rucker, C. Melander, P. B. Dervan, *Helv. Chim. Acta* **2003**, *86*, 1839–1851.
[59] K. A. Connors (Ed.), *Binding Constants*, Wiley & Sons, New York, Chichester, Brisbane, Toronto, Singapore, **1987**.
[60] J. R. Lakowicz, *Principles of fluorescence spectroscopy*, Plenum Press, New York, **1999**.

[61] All the compounds used in this paper were synthesized by the procedure described in ref.[49]
[62] In order to exclude the possibility of self association in the concentration range of the fluorescence studies (0.1–3 mM), a dilution experiment by UV and fluorescence spectroscopy in the buffer/7% (v/v) DMSO mixture was carried out with **4**, **9**, **10** and a **9/10** mixture (30:1) as models. The results showed that at ligand concentrations below 5×10^{-6} M all the ligands are monomers.
[63] The interstrand nOes suggested that sugar-oligoamides each present a certain percentage of hairpin conformation in the free state, and TR-NOESY also suggested hairpin structures in the bound state.
[64] S. Fery-Forgues, D. Lavabre, *J. Chem. Educ.* **1999**, *76*, 1260–1264.
[65] Under these conditions the sugar-oligoamide fluorescence quantum yield is at least ≈ 100% of its value in phosphate buffer solution. The refractive index of the aqueous buffer solution containing 7% (v/v) DMSO was therefore measured and the refractive index ratio was taken into account to determine the quantum yield for compound **4** and the models **1**–**3**, **9**–**10**.
[66] Studies on the solvent effect for indole fluorescence quantum yields show that changing the solvent from the apolar cyclohexane or methylcyclohexane to a polar and H-bonding solvent such as methanol or propan-2-ol produces a reduction of one order of magnitude in the fluorescence quantum yield value of the indole; a) S. C. Oh, Y. Shirota, *J. Photochem. Photobiol. A* **1995**, *92*, 79–83; b) J. J. Aaron, Z. Mechbal, A. Adenier, C. Parkanyi, V. Kozmik, J. Svoboda, *J. Fluoresc.* **2002**, *12*, 231–239; c) T. D. Nekipeiova, V. S. Shishkov, *High Energy Chem.* **2004**, *38*, 315–322; d) K. Guzow, J. Zielinska, K. Mazurkiewicz, J. Karolczak, W. Wiczk, *J. Photochem. Photobiol. A* **2005**, *175*, 57–68; e) G. Wenska, J. Koput, T. Pedzinski, B. Marciniak, J. Karolczak, B. Golankiewicz, *J. Phys. Chem. A* **2006**, *110*, 11025–11033.
[67] A dilution experiment with model compounds **1**–**3** was carried out in the 2×10^{-3} to 9×10^{-5} M concentration range. No chemical shift differences were detected, suggesting no aggregation behaviour.
[68] These nOes were also detected for sugar-oligoamides **4**, **6**–**7**; ref.[49]
[69] This enhancement of the fluorescence intensity has previously been used to quantify the interaction of other DNA binders. J. B. Chaires, *Methods in enzymology*, Academic Press, San Diego, USA, **2001**.
[70] Ligand concentration range from 1×10^{-6} M to 5×10^{-8} M and at different DNA concentrations [from 1×10^{-4} M to 3.2×10^{-3} M for *ct*-DNA, from 5×10^{-6} M to 2×10^{-5} M for *poly*(dA-dT), and at 1×10^{-3} M for *ml*-DNA].
[71] $\Delta\Delta G°$ **1** [*poly*(dA-dT) – *ct*-DNA] = –3.4 kcal mol^{-1}, $\Delta\Delta G°$ Im-Py-Py-γ-Py-Py-Py-Dp [(5′-TGTTA-3′) – (5′-AGAGT-3′)] = –2.7 kcal mol^{-1}.
[72] In order to confirm that the differences in the K_a values of the sugar-oligoamides are due to differences in the nature of the saccharide residue and not to cooperative binding, Hill plots for all the sugar oligoamide-*poly*(dA-dT) complexes were determined, and no cooperativity was found in any case (nH = 1); a) M. J. Jezewska, W. Bujalowski, *Biophys. Chem.* **1997**, *64*, 253–269; b) R. S. Cantor, *Biophys. J.* **1999**, *77*, 2643–2647; c) A. G. Kudrev, *J. Anal. Chem.* **2001**, *56*, 232–237; d) K. Matsuura, M. Hibino, T. Ikeda, Y. Yamada, K. Kobayashi, *Chem. Eur. J.* **2004**, *10*, 352–359; e) W. Bujalowski, *Chem. Rev.* **2006**, *106*, 556–606 (see Figure S23 in the Supporting Information).
[73] L. A. Marky, K. J. Breslauer, *Proc. Natl. Acad. Sci. USA* **1987**, *84*, 4359–4363.
[74] J. B. Chaires, *Biopolymers* **1997**, *44*, 201–215.
[75] G. Manzini, M. L. Barcellona, M. Avitabile, F. Quadrifoglio, *Nucleic Acids Res.* **1983**, *11*, 8861–8876.
[76] Comparisons are made with K_a values measured under conditions similar to ours: T = 20–27 °C, pH = 7.0–7.4, [NaCl] < 0.1 M.
[77] H. R. Drew, R. E. Dickerson, *J. Mol. Biol.* **1981**, *151*, 535–556.
[78] C. Giessnerprettre, B. Pullman, *Biochem. Biophys. Res. Commun.* **1982**, *107*, 1539–1544.
[79] M. Teng, N. Usman, C. A. Frederick, A. H. J. Wang, *Nucleic Acids Res.* **1988**, *16*, 2671–2690.
[80] This has been extensively studied; refs.[14,77–79]
[81] D. F. Eaton, *J. Photochem. Photobiol. B* **1988**, *2*, 523–531.
[82] D. F. Eaton, *Pure Appl. Chem.* **1988**, *60*, 1107–1114.
[83] S. Dhami, A. J. Demello, G. Rumbles, S. M. Bishop, D. Phillips, A. Beeby, *Photochem. Photobiol.* **1995**, *61*, 341–346.
[84] M. Gopal, M. S. Shahabuddin, S. R. Inamdar, *Proceedings of the Indian Academy of Sciences – Chemical Sciences* **2002**, *114*, 687–696.
[85] J. E. Larson, R. D. Wells, R. C. Grant, B. E. Shortle, C. R. Cantor, *J. Mol. Biol.* **1970**, *54*, 465–497.

Received: November 28, 2007
Published Online: ■

